

Bucknell University

Bucknell Digital Commons

Honors Theses

Student Theses

Spring 2023

Hygroscopic Tandem Differential Mobility Analyzer (HTDMA) Design and Testing for Aerosol Hygroscopic Behavior Studies

Ziheng Zeng
zz011@bucknell.edu

Follow this and additional works at: https://digitalcommons.bucknell.edu/honors_theses

 Part of the [Other Chemical Engineering Commons](#)

Recommended Citation

Zeng, Ziheng, "Hygroscopic Tandem Differential Mobility Analyzer (HTDMA) Design and Testing for Aerosol Hygroscopic Behavior Studies" (2023). *Honors Theses*. 632.
https://digitalcommons.bucknell.edu/honors_theses/632

This Honors Thesis is brought to you for free and open access by the Student Theses at Bucknell Digital Commons. It has been accepted for inclusion in Honors Theses by an authorized administrator of Bucknell Digital Commons. For more information, please contact dcadmin@bucknell.edu.

Hygroscopic Tandem Differential Mobility Analyzer (HTDMA) design and testing for aerosol hygroscopic behavior studies


by

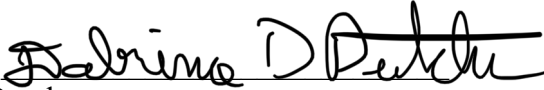
Ziheng Zeng

A Senior Thesis Submitted to the Honors Council
For Honors in Department of Chemical Engineering

April 24, 2023

Approved by:

Adviser: 
Timothy M. Raymond

Co-advisor: 
Dabrina D Dutcher

Acknowledgments

I want thank my research advisors, Dr. Tim Raymond and Dr. Dabrina Dutcher. This thesis was only completed with their assistance and dedicated involvement throughout the entire process. I am incredibly grateful for their support and understanding over the past three years and through the process of researching and writing this thesis. I would also like to express my gratitude to the faculty members of the Department of Chemical Engineering at Bucknell University for their assistance and support. Finally, I am thankful to my parents for their constant encouragement, support and unconditional love. I am also appreciative of my partner who supported me throughout this endeavor. This accomplishment would not have been possible without them. Thank you.

Table of Contents

| | |
|--|----|
| Acknowledgments | iv |
| Abstract | vi |
| Introduction | 1 |
| Experimental Method | 8 |
| 1. HTDMA instrumentation design | 8 |
| 1.1 Design of the HTDMA system | 8 |
| 1.2 Development of HTDMA software | 13 |
| 1.3 Calibration of HTDMA system | 15 |
| 2. Chemicals and hygroscopic growth measurements | 16 |
| 2.1 Single compound experiments | 16 |
| 2.2 Mixture experiments | 17 |
| Results and Discussion | 18 |
| 1. Assessment of the HTDMA instrumentation accuracy | 18 |
| 2. Single compound data evaluation | 19 |
| 3. Mixtures of compounds data evaluation | 25 |
| Conclusions and Future work | 32 |
| Bibliography | 34 |
| Appendix | 36 |
| A1. An example of full size distribution obtained from one DMA | 36 |
| A2. An example of selected narrow-range size distribution obtained from TDMA | 37 |

Abstract

Most particles in the atmosphere take up water when exposed to increasing relative humidity (RH), and this behavior is described and quantized by a hygroscopicity parameter, κ . Hygroscopic Tandem Differential Mobility Analysis (HTDMA) can be used to measure the physicochemical properties of aerosol particles and study phenomena that lead to size changes in submicron aerosol particles. Specifically, HTDMA measures how aerosol particles of different initial dry sizes grow or shrink when exposed to changing RH. HTDMA uses two differential mobility analyzers (DMAs) and a humidification system to make these measurements. One DMA selects a narrow size range of dry aerosol particles which are exposed to varying RH conditions in the humidification system. The second humidified DMA scans the particle size distribution after the particles have been conditioned by the humidification system. Scanning a wide range of particle sizes enables the second DMA to measure changes in size or growth factor (growth factor = humidified size/dry size) due to water uptake by the particles. The κ can then be calculated from the growth factor. A new HTDMA system was designed for a set of RH conditions with user-friendly data-analyzing software. The software can determine the theoretical distribution of dry particles and accurately captures multiple peaks even in the presence of "shoulders", i.e. when two peaks are close in diameter. A user interface was designed using the Qt library in Python, allowing the user to explore the fitted data. The designed HTDMA system was calibrated by pure ammonium sulfate, a well-characterized salt that can be used to calibrate these systems. The hygroscopic behavior of a few pure amino acids and aerosol mixtures of amino acids and ammonium sulfate was investigated. Initial results indicate that L-proline is moderately hygroscopic, L-leucine is non-hygroscopic, L-valine is only slightly hygroscopic for larger sizes, and 2-Methylglutaric Acid (2MGA) is only slightly hygroscopic.

The mixture of proline and ammonium sulfate is moderately hygroscopic on the high end over all other mixtures. The mixtures of proline + 2MGA, leucine + ammonium sulfate, valine + ammonium sulfate are moderately hygroscopic on the low end. The mixture of leucine and 2MGA is non-hygroscopic. For the mixture of valine and 2MGA, smaller sizes are non-hygroscopic, while larger sizes are moderately hygroscopic on the low end. Although some findings were observed based on the initial results, more experiments are required to increase the repeatability of these results and to be more accurate and conclusive on the hygroscopic properties of studied aerosol particles.

Introduction

In recent decades, the role of aerosol particles in understanding climate change and developing climate models has received much more attention. Researchers have a growing interest in observing and characterizing the sources, sinks and understanding atmospheric complexity (Kreidenweis and Asa-Awuku, 2014). In fact, organic aerosols, tiny particles composed of carbon and other organic molecules suspended in the atmosphere, are made up of 20% to 50% of the total fine aerosol mass in the United States and around 10 to 75% of the organic carbon are water-soluble (Moore and Raymond, 2008). When organic aerosols are exposed to moist air, or relative humidity (RH), they can absorb water molecules onto their surface, leading to an increase in their size and mass. A graphic illustration of such growth, called hygroscopic growth, is shown in **Figure 1**.



Figure 1. Schematic illustration of aerosol hygroscopic growth, where the "wet particle" is shown as a core-shell, but most particles won't physically look like it (Department of Environmental Science, Stockholm University).

The hygroscopic growth of an aerosol particle can be determined by its chemical composition, size, and shape (Kreidenweis and Asa-Awuku, 2014). Different compounds can exhibit varying degrees of water uptake depending on their chemical composition and size. For example, soluble

aerosol particles are typically more hygroscopic than particles consisting of insoluble materials. The size and shape of the aerosol particle can also affect its hygroscopic properties, as larger and more irregularly shaped particles tend to absorb more water vapor than smaller and more spherical particles (Petters and Kreidenweis, 2007). Studies have shown that generally particles that have taken on water and are suspended in a liquid or air will tend to become spherical in shape due to surface tension (Banavar & Maritan, 2010). Thus, in this study, particles are assumed to be spherical to reduce the complexity of the problem. Therefore, the size change in diameter of different aerosol particles caused by increasing humidity is focused on in this research.

The Kohler effect describes the relationship between the relative humidity of an aerosol particle and its size. Specifically, it characterizes how much the particle grows depending on the relative humidity of the environment (Petters and Kreidenweis, 2007). The Kohler curve, from Kreidenweis and Asa-Awuku (2014), shown in **Figure 2**, shows how the aerosol particle grows very little at lower humidity, but the particle increases greatly in size at higher relative humidity. Once the aerosol particles reach a threshold of very high supersaturation, they will grow rapidly to form very large-sized droplets. For our research purpose, we are only interested in a relative humidity of 0% - 100% RH (indicated using the red box in **Figure 2**) and particles that have a size of around 0.01-1 μm (typical size of aerosol particles).

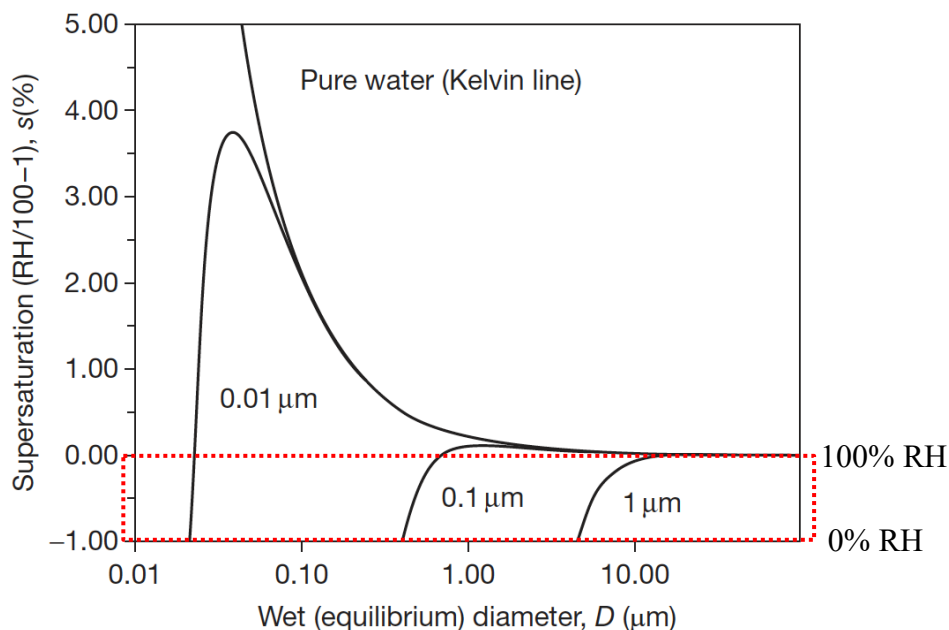


Figure 2. Sample calculated Kohler curves: variation of the equilibrium drop size with the saturation ratio for pure ammonium sulfate, with the dry radius labeled in units of microns.

To quantify the size change in the diameter of aerosols, a growth factor (GF) is commonly used, which is a ratio of the humidified size in diameter to the initial dry size in diameter of the particle (Rader and McMurry, 1986). It can be written as **Eq. (1)**.

$$\text{growth factor (GF)} = \frac{\text{humidified size in diameter (nm)}}{\text{dry size in diameter (nm)}} \quad (1)$$

A relationship between growth factor and relative humidity of the aerosols can be then plotted as **Figure 3**, based off from the Kohler curve, in the interested region of RH and particle size of 0.01-1 μm.

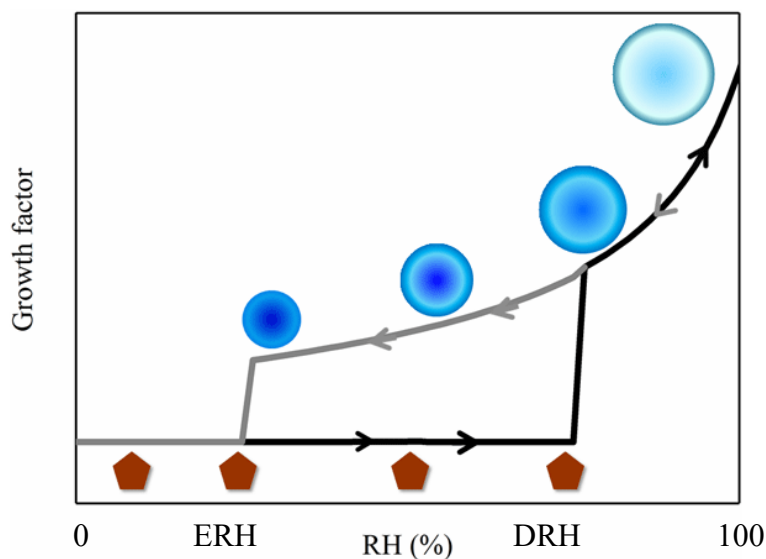


Figure 3. Theoretical curve characterizing the relationship between RH and aerosol growth factor, where the black curve is the hydration line and the gray curve is the dehydration curve (DRH = deliquescence relative humidity & ERH = efflorescence relative humidity) (Tang et al., 2019).

The black curve shows that as the RH increases, the aerosol particles can start to grow once reach a certain point (DRH), where an aerosol particle becomes fully soluble in water vapor and starts to dissolve. The gray curve indicates that once the aerosols start to absorb water and grow in size, they will decrease in size, following along the gray line until they reach another point (ERH), at which a saturated solution of a salt or other solid material loses water molecules to the surrounding air, resulting in the formation of a dry powder. While different chemicals have different values for DRH and ERH, and they affect the behavior of hygroscopic growth, this research is not interested in finding the values of DRH and ERH for different chemicals. Instead, we are interested in curvy the part of the line where the particle starts to absorb water and grow

in size and shrink when gets dehydrated, as well as the relationship between the growth and relative humidity.

To quantify the hygroscopic growth, Petters and Kreidenweis (2007) proposed a hygroscopicity parameter (denoted by κ , Kappa) to be used as a measurement. The hygroscopic parameter Kappa (κ) is a dimensionless quantity that describes the water vapor absorption properties of atmospheric aerosols (Kreidenweis and Asa-Awuku, 2014). The value of Kappa depends on the composition, size, and shape of the aerosol particle, as well as the environmental conditions including temperature and RH. Aerosol particles with higher Kappa values are more hygroscopic, meaning they can absorb more water vapor from the surrounding air before reaching saturation. Aerosol particles with κ values between 0.2 and 0.6 are generally considered to be moderately hygroscopic, while those with κ values greater than 0.6 are highly hygroscopic. Aerosol particles with Kappa (κ) values below 0.2 are generally considered to be non-hygroscopic or only slightly hygroscopic. Based on the correlation between water activity and Kappa developed by Petters and Kreidenweis (2007), Kreidenweis and Asa-Awuku (2014) rearranged the original equation and obtained a simplified equation expressing Kappa as a function of GF and RH, shown in **Eq. (2)**. This equation will be used in our study to calculate the the Kappa for different aerosol compounds based on the operating conditions RH and calculated GF.

$$kappa (\kappa) = \frac{GF^3 - 1}{RH/(1 - RH)} \quad (2)$$

The hygroscopic growth of aerosol particles can affect the way they interact with light, scatter radiation, and influence cloud formation and precipitation patterns (Kreidenweis and Asa-

Awuku, 2014). When these aerosols become hydrated, they can act as cloud condensation nuclei (CCN), which are small particles that serve as the basis for cloud droplet formation. Specifically, the size, composition and hygroscopicity of aerosol particles can affect their effectiveness as CCN and their impact on cloud formation, which can then affect cloud reflection, lifetime, and precipitation patterns. Additionally, the abundance and distribution of hygroscopic aerosols in the atmosphere can affect the formation, duration, and properties of clouds (Sorooshian et al., 2009). Eventually, the size change of aerosol particles can affect weather patterns and climate. While water-soluble organic aerosols are relatively abundant, the hygroscopic properties of organic aerosols and their mixtures are poorly understood (Cruz and Pandis 2000). Therefore, understanding the hygroscopic properties of organic aerosols is important for predicting their behavior in the atmosphere and their impact on climate and air quality.

Prior research has shown that an Hygroscopic Tandem Differential Mobility Analysis (HTDMA) can be used to measure the physicochemical properties of aerosol particles and study phenomena that lead to size changes in submicron aerosol particles (Rader and McMurry, 1986). Specifically, HTDMA uses two in-series DMAs (TDMA) and one humidification system to measure how aerosol particles of different initial dry mobility sizes (which assumes spherical particles) grow or shrink when exposed to changing relative humidity (Moore and Raymond, 2008). The first DMA selects a narrow size range of dry aerosol particles exposed to varying RH conditions in the humidification system. The second humidified DMA scans the particle size distribution after the humidification system has conditioned the particles. Scanning a wide range of particle sizes enables the second DMA to measure changes in size or growth factor due to water uptake by the particles, where the growth factor can be calculated using **Eq. (1)**. Overall, the HTDMA technique can effectively detect small changes in particle diameter as result of

increased RH and subsequent water-uptake by a size-selected aerosol sample (Kreidenweis and Asa-Awuku, 2014).

Although commercial HTDMA is available for purchase, it is extremely expensive (where high-end models costs \$150,000 or more), complicated to use, and limited to certain types of aerosols, and requires frequent calibration by the manufacturer. To avoid all the cost, complexity and restriction of using a commercial HTDMA, and to effectively study the hygroscopic properties of organic aerosols, an HTDMA system with RH control system was researched, built, and calibrated based on work by Cruz and Pandis (2000) and Brechtel and Kreidenweis (2000). New HTDMA software was also developed to analyze the data on detecting and fitting size distribution peaks.

Additionally, the hygroscopicity behavior of several singles and mixtures of selected aerosols was studied. As part of Professors Dutcher and Raymond's on-going NSF-funded research on "the role of interactions between organic components on aerosol hygroscopicity", ammonium sulfate as a non-surface-active compound and 2-Methylglutaric Acid (2MGA) as a surface-active compound were selected to mix with common amino acids (L-Proline, L-Leucine, and L-Valine) which are organic compounds that might contribute to the formation of aerosols and clouds under some circumstances..

In this article, firstly, the experimental methods used in building the HTDMA system will be explained, as well as the procedures used to quantify the hygroscopicity of various chemical compounds and mixtures of aerosol compounds. Later, the article will assess the effectiveness of the designed HTDMA system, and evaluate the resulting hygroscopicity of the studied chemical compounds and mixtures. Finally, conclusions will be made based on the initial experimental results and future works will be recommended.

Experimental Method

1. HTDMA instrumentation design

1.1 Design of the HTDMA system

Firstly, two differential mobility analyzers (DMAs) are used for an HTDMA system. DMAs are devices used to measure and separate particles of different sizes based on their electrical mobility. Electrical mobility refers to the velocity at which a particle moves in response to an applied electric field (Fuchs, 1989). This velocity is related to the electrical charge and size of the particle, as well as the strength and direction of the electric field.

The principle of operation of a DMA is based on the fact that particles of different sizes and charges will move at different rates in an electric field (Wang et al., 2011). A typical DMA consists of two main parts: a cylindrical inner electrode and a coaxial outer electrode. The electrodes are separated by a narrow annular gap, through which the sample particles flow. The inner electrode is held at a high voltage, creating an electric field that causes the particles to move towards it. The outer electrode is grounded and provides a return path for the electric current. **Figure 4a** below shows a schematic diagram of a DMA with flow directions in the DMA.

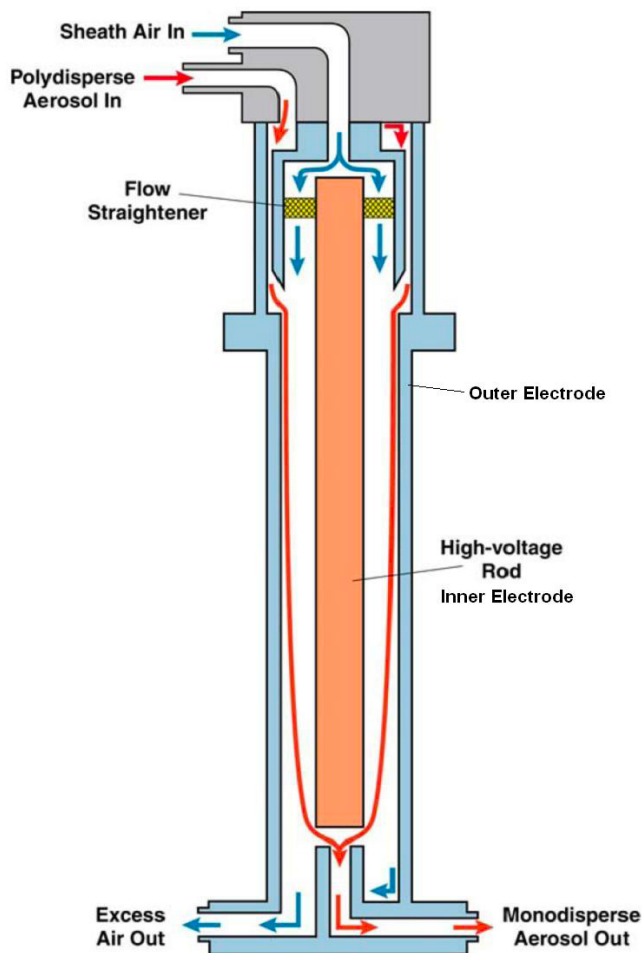


Figure 4a. Differential mobility analyzer (TSI operation manual)

As the particles move through the DMA, they experience a drag force due to the surrounding air, which balances the electric force and gravitational force. The size and charge of each particle determine the strength of the drag force and hence the velocity at which it moves. The DMA measures the particle mobility by analyzing the current flowing between the electrodes, which is proportional to the number of particles passing through the gap. To separate particles of different sizes, a sheath flow of air is introduced into the annular gap, perpendicular to the sample flow. This creates a laminar flow pattern, which causes particles to move towards the inner electrode at different rates, depending on their size and charge. The smaller particles

move more slowly and tend to follow the air streamlines more closely, while the larger particles move faster and tend to deviate from the streamlines. An example flow diagram is shown in **Figure 4b**. By adjusting the voltage and flow rate of the sheath air, the DMA can be used to select particles of a specific size range.

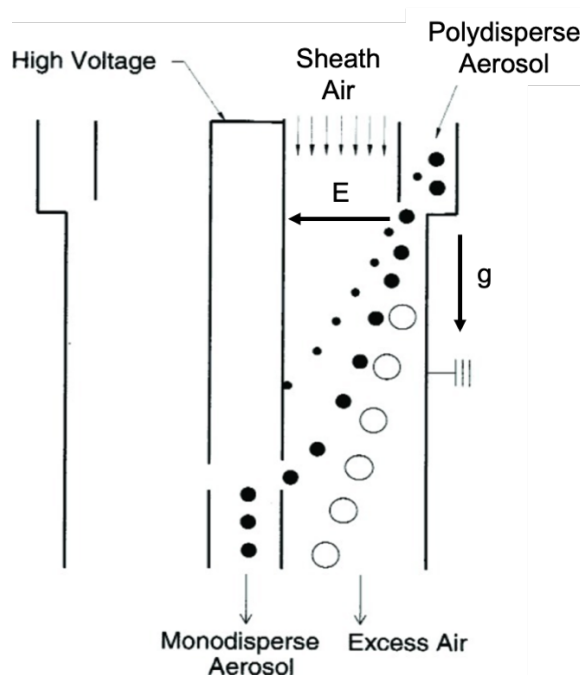


Figure 4b. Schematic diagram for a gas flow in a differential mobility analyzer (edited on diagram from Mulholland et al., 2006).

A TDMA (tandem differential mobility analyzer) system was built by connecting two differential mobility analyzers (DMAs), as shown in **Figure 5**. Solution with the chemical compound interested is injected from a syringe pump into an atomizer (3076, TSI) to aerosolize the interested compound. After going through a silica gel diffusion dryer, the dry aerosol particles enter the first DMA (DMA 3080, TSI), where it selects a narrow size range of dry aerosol particles from a full-size distribution. Then the selected particles enter the second DMA (DMA 3080, TSI), where it scans the particle size distribution after the particles. Examples of a

full-size distribution and selected narrow-range size distribution are included in Appendix A1 and A2. A condensation particle counter (CPC 3775, TSI) downstream of the second DMA counts particles to generate size distribution.

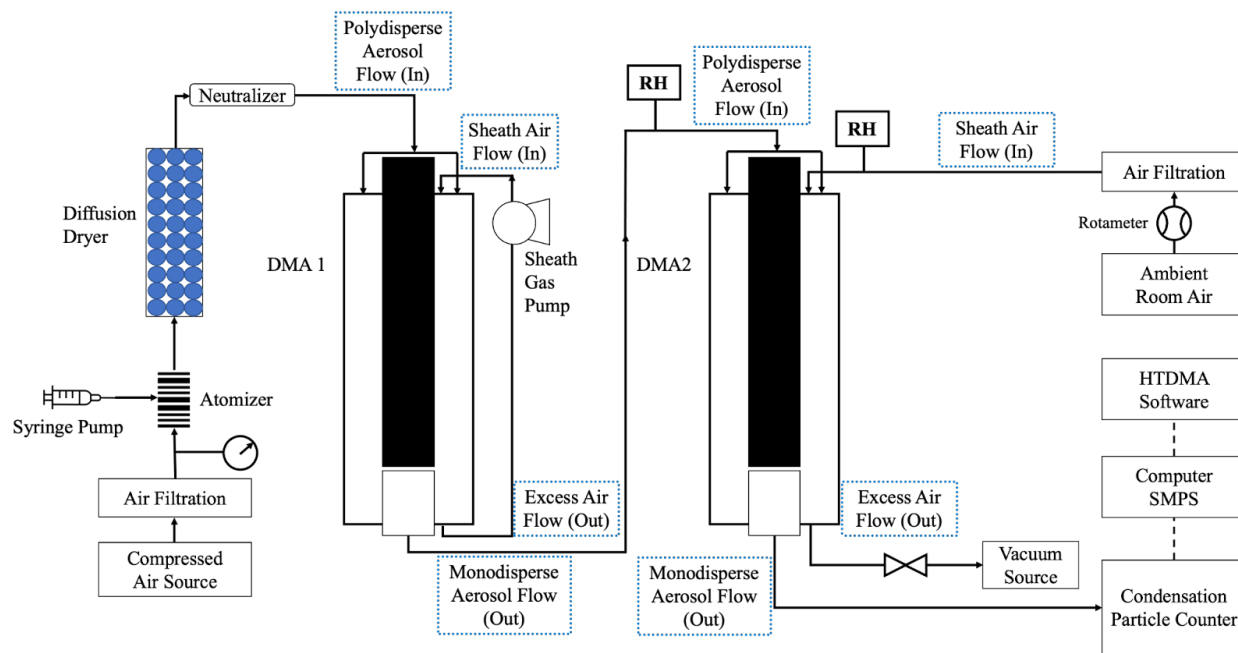


Figure 5. TDMA design scheme.

Then, to build an HTDMA (hygroscopic tandem differential mobility analyzer) system, a humidification system with controllable relative humidity (RH), shown in **Figure 6**, was incorporated into the TDMA system. The dry flow line is first humidified to maximum RH using a humidifier, then dry airflow is introduced into the humidified flow line to reduce the RH to the desired. The humidifiers used in the lab were PermaPure Nafion Tube (MH-110-12P-4) and PermaPure Humidifier (FC-100-80). These humidifiers have semi-permeable membranes that allow water vapor to pass through while blocking larger water molecules from entering the aerosol flow. In this process, water is placed on one side of the semi-permeable membrane, and aerosol flow is passed over the other side, as shown in **Figure 6**. The aerosol flow becomes

humidified as it absorbs the water vapor passing through the humidifier. Both humidifiers have a maximum relative humidity (RH) at around 90% for the operated flow rates. Introducing dry air into the humidified flow can reduce the humidity in the flow. By switching the dry air flow control valve, we were able to control the dry airflow and thus reduce the RH to desired values. An RH meter (Vaisala HM 70) was inserted into the mixed flow line to monitor the real-time relative humidity.

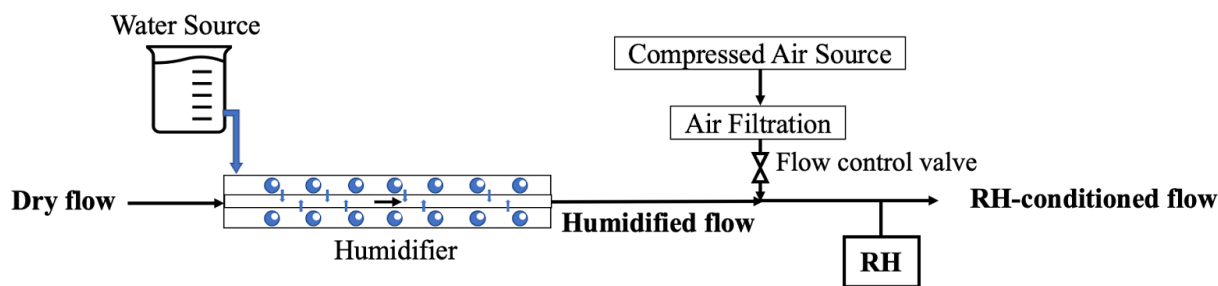


Figure 6. Humidification system scheme.

The finalized design of HTDMA is shown in **Figure 7**, consisting of two DMAs and one humidification system. Similar to a TDMA system, for an HTDMA system, the first DMA selects a narrow size range of dry aerosol particles exposed to varying RH conditions in the humidification system. The second humidified DMA scans the particle size distribution after the humidification system has conditioned the particles. The sheath-to-aerosol flow rate ratio was maintained for both DMAs at 10:1, which is the optimal ratio for keeping flows laminar.

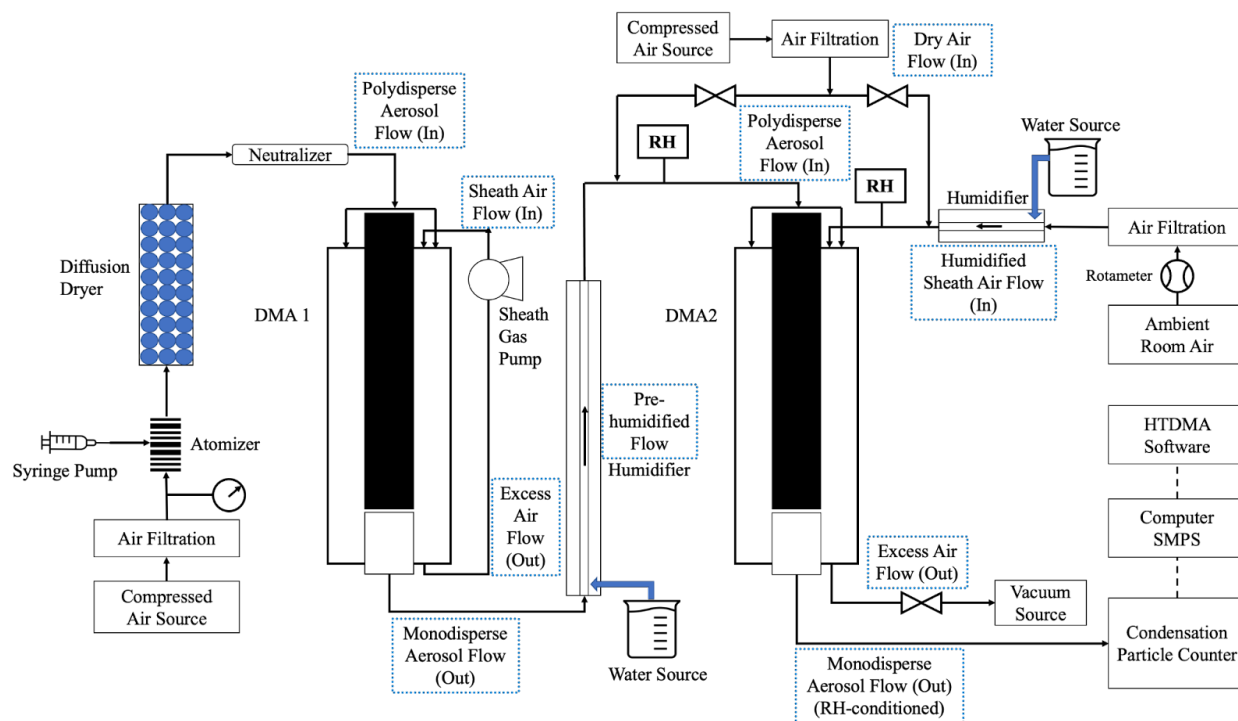


Figure 7. HTDMA design scheme.

A condensation particle counter (CPC) downstream of the second DMA counts particles as a function of selected sizes to obtain the size distribution of RH-conditioned particles. The data is then imported into the HTDMA software, explained in the next section, to fit the peaks of the dry size diameter and the humidified size diameter. Once the peaks of the dry diameter and wet diameter are fitted using the software, we can use the size values to calculate the growth factor (GF) using **Eq. (1)**. Then, the hygroscopicity (κ value) can be calculated using **Eq. (2)** (Kreidenweis and Asa-Awuku, 2014).

1.2 Development of HTDMA software

New HTDMA software was also developed to analyze the data on aerosol hygroscopicity. The software uses supplied parameters to determine the theoretical distribution of dry particles while performing a least squares fit using a curve that is designed to fit multiple

Gaussian distributions on a log-normal scale. Our approach accurately captures multiple peaks even in the presence of "shoulders", i.e. when two peaks are close in diameter, as shown in **Figure 9** below. A user interface (**Figure 8**) was designed using the Qt library in Python, allowing the user to explore the fitted data.

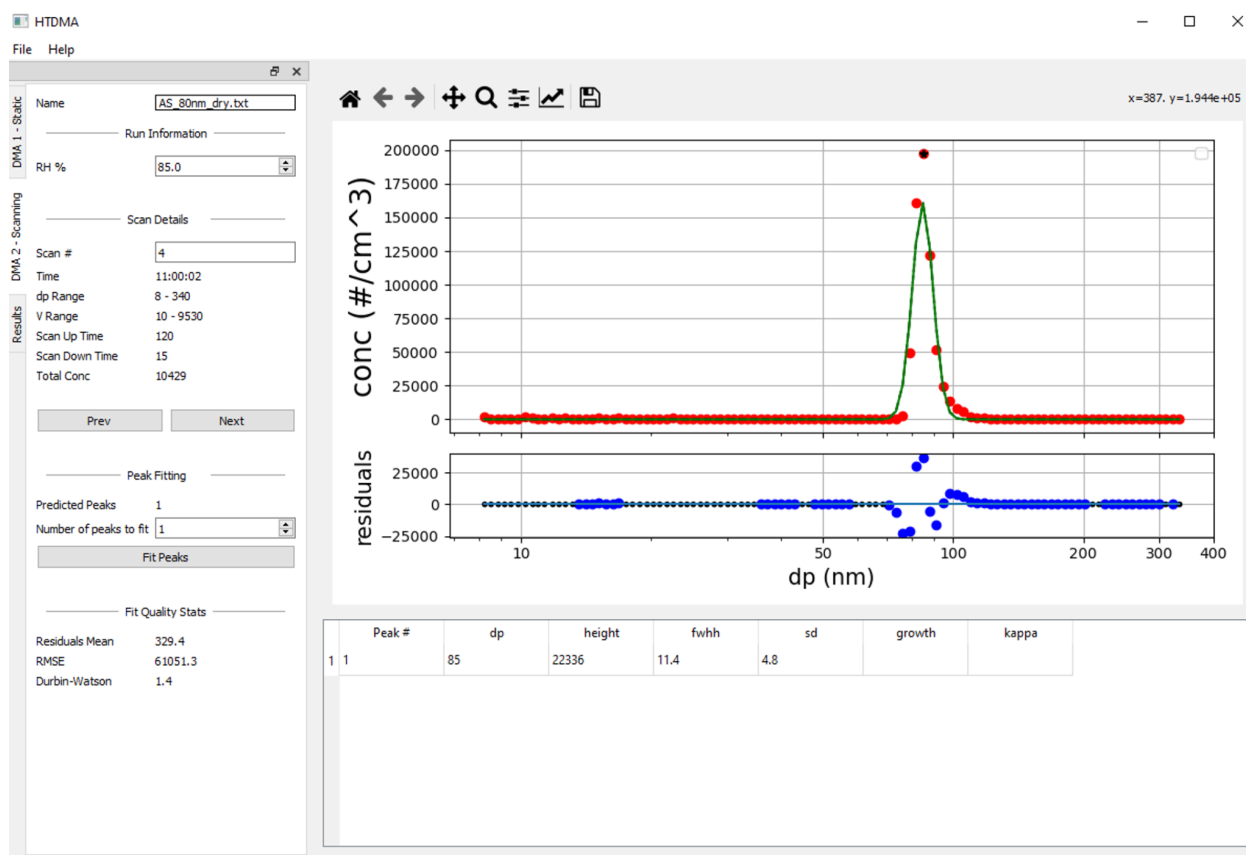


Figure 8. HTDMA software user interface.

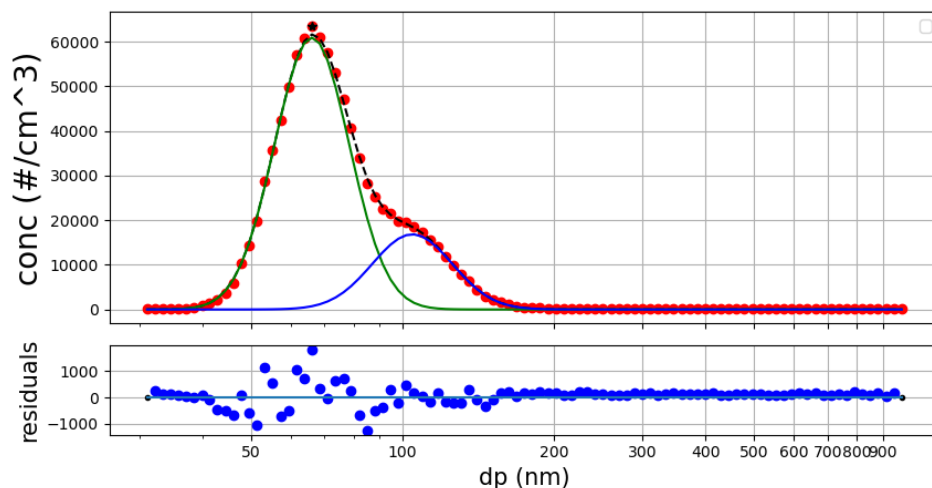


Figure 9. Example of “shoulder” peaks fit.

1.3 Calibration of HTDMA system

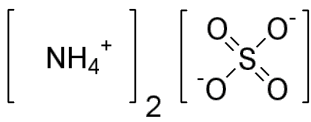
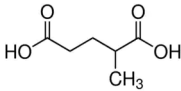
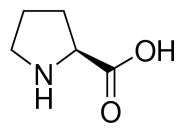
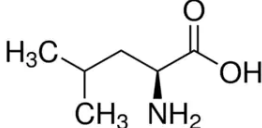
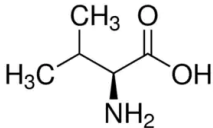
Finally, the HTDMA system was calibrated using ammonium sulfate (solution with a concentration of 0.1g/L) idealized curve from Taylor et al., 2011. Specifically, the aerosolized ammonium sulfate was introduced into the system under varying RH conditions, including RHs of below 10%, 40%, 60%, 70%, and 80%. The data was then analyzed using the HTDMA software to get a growth factor (GF) to compare with the idealized curve from the literature. If the experimental data points fall onto the curve perfectly, the HTDMA is successfully functioning under different RH conditions.

2. Chemicals and hygroscopic growth measurements

2.1 Single compound experiments

The single pure compound (~98% purity) of chemicals was investigated using the HTDMA system to study the hygroscopic growth behavior. The list of chemicals and properties studied is shown in **Table 1**.

Table 1. Chemical compounds explored in experiments.

| Compound | Chemical Formula | Molecular Weight (g/mol) | Solubility in water at 25°C (g/L) | Molecular Structure |
|------------------------------|--------------------------------------|--------------------------|-----------------------------------|---|
| Ammonium Sulfate | $(\text{NH}_4)_2\text{SO}_4$ | 132.14 | 770 ^[1] |  |
| 2-Methylglutaric Acid (2MGA) | $\text{C}_6\text{H}_{10}\text{O}_4$ | 146.14 | 40.6 ^[2] |  |
| L-Proline | $\text{C}_5\text{H}_9\text{NO}_2$ | 115.13 | 1623 ^[1] |  |
| L-Leucine | $\text{C}_6\text{H}_{13}\text{NO}_2$ | 131.17 | 22.4 ^[1] |  |
| L-Valine | $\text{C}_5\text{H}_{11}\text{NO}_2$ | 117.15 | 85 ^[1] |  |

[1]chembk.com, [2]hmdb.ca

To perform the HTDMA measurements, the solutions of each chemical were made with a concentration of 0.1 g/L. Aerosol particles of each chemical were generated using the atomizer and introduced into the HTDMA system to get the final GF and Kappa values, as described in

earlier sections. The experiments for every single compound were repeated under a variety of size settings on the first DMA (30 nm, 50 nm, 80 nm, and 100 nm) and different system RH conditions (30%, 50%, 70%, and 90%). The hygroscopicity (Kappa value) was then calculated using **Eq. (2)**, based on RH and the GF calculated from different settings.

2.2 Mixture experiments

The mixtures of chemicals, which are not as well characterized as pure ammonium sulfate, were also investigated using the HTDMA system to study the hygroscopic growth behavior. The experimental samples of mixtures were made of 50:50 weight percent of compound 1 (L-Proline, L-Leucine, L-Valine) and compound 2 (Ammonium sulfate, 2MGA), respectively, at a concentration of 0.1g/L. A list of experimented mixtures is presented in **Table 2** below.

Table 2. Mixtures of chemicals explored in experiments.

| Mixture No. | Compound 1 | Compound 2 | Ratio |
|-------------|------------|------------------------------|-------|
| 1 | L-Proline | Ammonium Sulfate | 50:50 |
| 2 | L-Proline | 2-Methylglutaric Acid (2MGA) | 50:50 |
| 3 | L-Leucine | Ammonium Sulfate | 50:50 |
| 4 | L-Leucine | 2-Methylglutaric Acid (2MGA) | 50:50 |
| 5 | L-Valine | Ammonium Sulfate | 50:50 |
| 6 | L-Valine | 2-Methylglutaric Acid (2MGA) | 50:50 |

The experiments for every mixture were repeated under a variety of size settings on the first DMA (30 nm, 50 nm, 80 nm, and 100 nm) and different system RH conditions (30%, 50%,

70%, and 90%). The hygroscopicity (Kappa value) was then calculated using Eq. (2), based on RH and the GF calculated from different settings.

Results and Discussion

1. Assessment of the HTDMA instrumentation accuracy

To assess the functionality and accuracy of the HTDMA instrumentation, calibration using a well-characterized salt ammonium sulfate was done as described in the method section, and the result of experimental data points superimposed onto the idealized curve is shown in

Figure 10.

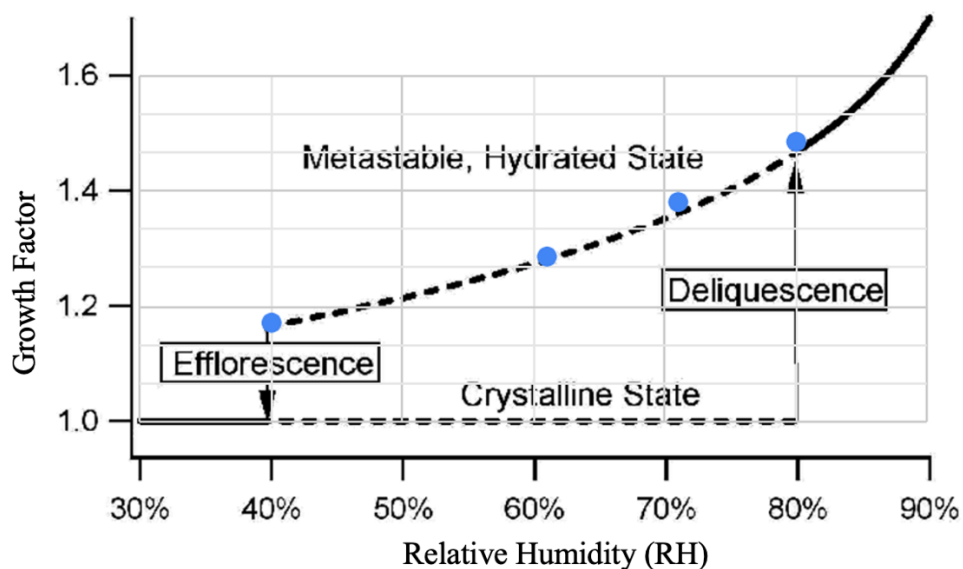


Figure 10. Experimental data (blue dots) superimposed on the ammonium sulfate idealized curve (Taylor et al., 2011).

As shown in **Figure 10**, the experimental data of the ammonium sulfate growth factor (shown in blue dots) aligns almost perfectly with the idealized curve. This shows that the designed system works successfully to characterize the growth behavior of aerosol particles.

2. Single compound data evaluation

The calculated Kappa values for studied chemicals are listed in **Table 3**. Some theoretical values for Kappa found in the literature for corresponding chemicals are also included in the table for comparison.

Table 3. Kappa values of single compounds.

| Compound | Experimental Kappa | Theoretical Kappa |
|------------------|--------------------|----------------------------------|
| L-Proline | 0.42 ± 0.14 | N/A |
| L-Leucine | 0.04 ± 0.10 | 0.002 (Raymond and Pandis, 2003) |
| L-Valine 1* | -0.02 ± 0.02 | N/A |
| L-Valine 2* | 0.16 ± 0.06 | N/A |
| 2MGA | 0.16 ± 0.03 | 0.154 (Huff Hartz et al., 2006) |
| Ammonium Sulfate | 0.65 ± 0.11 | 0.61 (Clegg and Wexler, 1998) |

Note. For L-valine, two adjacent size peaks were observed (**Figure 9** is an example) for particles size-selected at 80 nm and 100 nm and only one peak was observed for particles size-selected at 30 nm and 50 nm. To indicate the difference, L-Valine 1 Kappa was calculated from particle size-selected at 30 nm, 50 nm, and the first peak for 80 nm and 100 nm; L-Valine 2 was calculated from the second peak of particles size-selected at 80 nm and 100 nm.

The initial results of tabulated experimental Kappa indicate that L-proline is a moderately hygroscopic particle with a Kappa at 0.42 ± 0.14 . L-leucine is a relatively non-hygroscopic particle with a Kappa close enough to zero, which is also indicated by the literature value. For

valine, we observed a double peak of hydrated growing particles for particle size selected at 80 nm and 100 nm, which is unusual. This might be due to that valine has different dry crystal structures that will rearrange differently into different spherical sizes when absorb water. However, this is an odd observation and more repeated runs of different sizes are needed to yield a more conclusive result. To account for the observed two sizes, two different Kappas were calculated based on the smaller and the larger size, and the specifics were explained in the notes below in **Table 3**. The smaller peak shows that L-valine is not a hygroscopic particle with a Kappa close to zero, while the larger size peak tells us that there is some portion of the larger size L-valine did take up some water and grew in their size, with a Kappa of 0.16 ± 0.06 . For 2MGA, the Kappa is calculated to be 0.16 ± 0.03 , close to the literature value, indicating that it is only slightly hygroscopic particle. Lastly, for ammonium sulfate, which was a well-characterized hygroscopic salt used for the calibration of the HTDMA system, a Kappa of 0.65 ± 0.11 was obtained. This Kappa value is close to the literature value of 0.61 and also shows that ammonium sulfate is highly hygroscopic compared to all of the other experimented chemicals.

Since the experiment directly measured the growth factor, and the Kappa was calculated from **Eq. (2)**, both growth factor and Kappa versus RH plots for each compound are made, as shown in **Figure 11 - 14**, to determine if a trend can be observed.

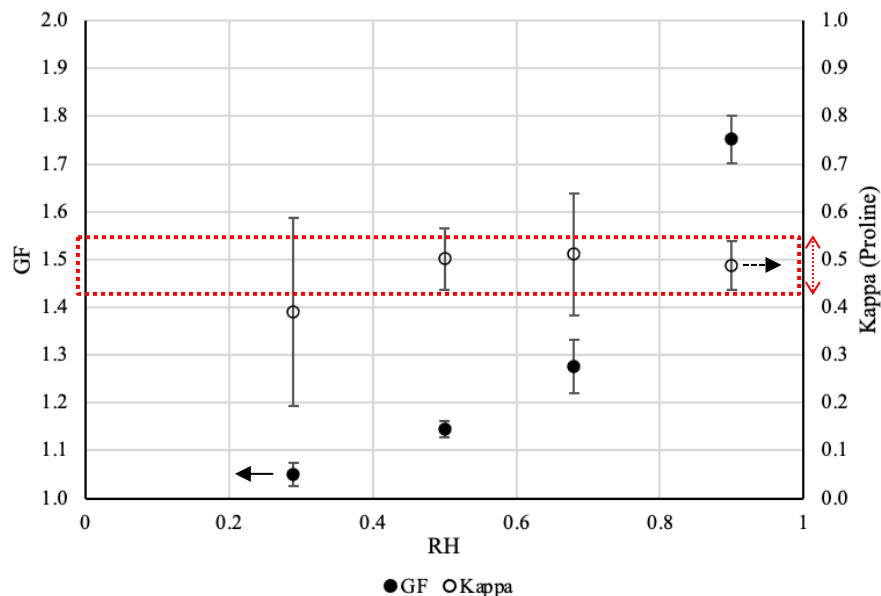


Figure 11. Growth factor (GF) and Kappa vs. RH plot for pure proline, where the solid dots are the GF values (reading from the right to the left indicated by the arrow, on the primary y-axis) and the hollow dots are the Kappa values (reading from the left to the right, on the secondary y-axis). The error bars represent one standard deviation, and red dashed box indicates likely Kappa range.

From **Figure 11**, we can see that for proline, the growth factor is increasing with as RH increases, and this positive correlation matches the hygroscopic growth curve shown in **Figure 3**. This reinforces the proline is a moderately hygroscopic aerosol particle. The average Kappa value for proline was calculated to be 0.42 ± 0.14 , but varies slightly at a different relative humidity, as shown in **Figure 11**. Although one compound theoretically has one constant Kappa value, our experiments yielded a small range of values, but still close to one constant Kappa value if taking account of the experimental errors and the assumption of spherical particles.

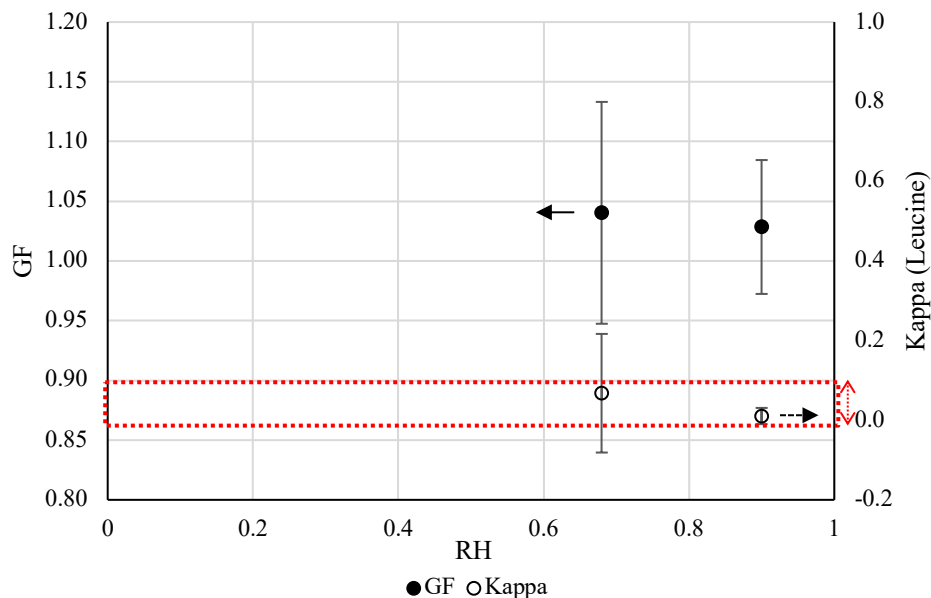


Figure 12. Growth factor (GF) and Kappa vs. RH plot for pure leucine, where the solid dots are the GF values (reading from the right to the left indicated by the arrow, on the primary y-axis) and the hollow dots are the Kappa values (reading from the left to the right, on the secondary y-axis). The error bars represent one standard deviation, and red dashed box indicates likely Kappa range.

From **Figure 12**, we can see that for leucine, no growth was observed as there is no positive correlation between GF and RH, indicating that leucine is non-hygroscopic. Similar to proline, our experiments yielded a small range of Kappa values for leucine, but the value is still close to one constant Kappa value if taking into account of the experimental errors and the assumption of spherical particles. In addition, although negative Kappa value is not physically meaningful, it is possible when a non-spherical particle becomes more spherical as it absorbs water, resulting in a decrease in the measured diameter and negative Kappa.

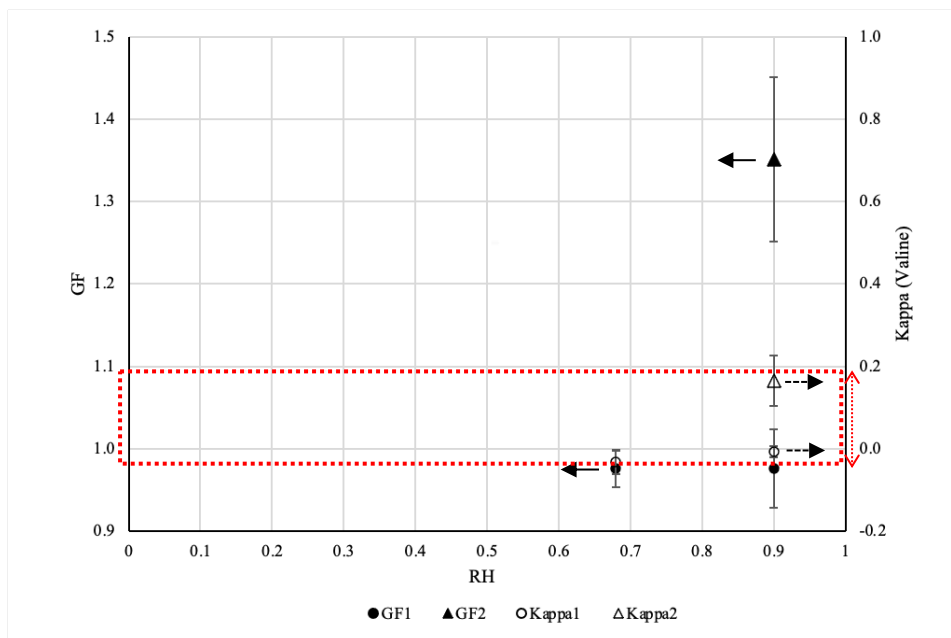


Figure 13. Growth factor (GF) and Kappa vs. RH plot for pure valine, where the round solid dots (GF 1) are the GF values for smaller sizes (reading from the right to the left indicated by the arrow, on the primary y-axis) and the triangular solid dot (GF 2) is the GF for bigger size; while the round hollow dots (Kappa 1) are the Kappa values for smaller sizes (reading from the left to the right, on the secondary y-axis) and the triangular hollow dot (Kappa 2) is the Kappa for bigger size. The error bars represent one standard deviation, and red dashed box indicates possible Kappa range.

From **Figure 13**, we can see that for valine, no growth was observed as there is no positive correlation between GF and RH for smaller particles, indicating that most of the smaller particles of valine are non-hygroscopic. However, we observed some growth for larger particles of valine, as denoted below **Table 3**, meaning that large sizes of valine are only slightly hygroscopic. More experiments on different sizes of valine need to be done to be able to know the threshold size for non-hygroscopic and hygroscopic valine particles.

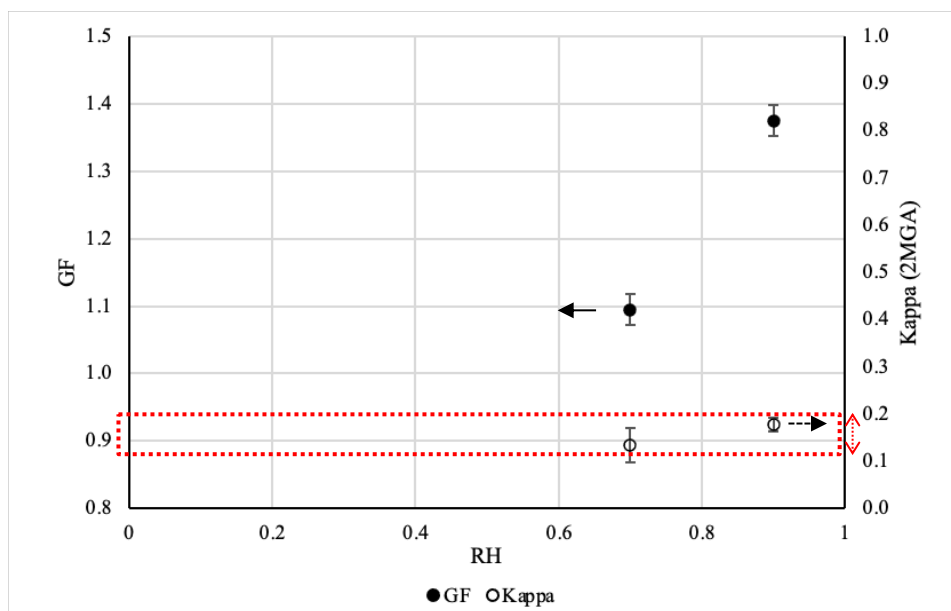


Figure 14. Growth factor (GF) and Kappa vs. RH plot for pure 2MGA, where the solid dots are the GF values (reading from the right to the left indicated by the arrow, on the primary y-axis) and the hollow dots are the Kappa values (reading from the left to the right, on the secondary y-axis). The error bars represent one standard deviation, and red dashed box indicates likely Kappa range.

From **Figure 14**, we can see that for 2MGA, the growth factor increases slightly as RH increases, and this positive correlation matches the hygroscopic growth curve shown in **Figure 4**. This reinforces the 2MGA is a slightly hygroscopic aerosol particle. The average Kappa value for proline was calculated to be 0.16 ± 0.03 , but varies slightly at a different relative humidity as shown in **Figure 14**.

Overall, based on the initial experimental data, proline is a moderately hygroscopic particle, leucine is non-hygroscopic, and 2MGA is slightly hygroscopic. For valine, smaller particles are non-hygroscopic, while larger particles are slightly hygroscopic. As explained before, it is possible that valine has several different dry crystal structures that will rearrange

differently into different spherical sizes when absorb water. However, more repeated runs at the same settings and additional runs at different sizes and relative humidity are required to be more accurate and conclusive on the hygroscopic properties of those particles.

3. Mixtures of compounds data evaluation

The calculated Kappa values for studied mixtures are listed in **Table 4**.

Table 4. Kappa values of mixtures, where Ammonium sulfate is abbreviated as AmmSulf.

| Mixture | Experimental Kappa | Standard Deviation |
|-------------------|--------------------|--------------------|
| Proline + AmmSulf | 0.50 | 0.03 |
| Proline + 2MGA | 0.21 | 0.10 |
| Leucine + AmmSulf | 0.29 | 0.13 |
| Leucine + 2MGA | -0.04 | 0.04 |
| Valine + AmmSulf | 0.27 | 0.12 |
| Valine + 2MGA 1* | -0.08 | 0.07 |
| Valine + 2MGA 2* | 0.29 | 0.07 |

Note. For L-Valine + 2MGA mixture, two size peaks was observed for particles size-selected at 50 nm and 80 nm and only one peak was observed for particles size-selected at 30 nm. To indicate the difference, L-Valine + 2MGA 1 Kappa was calculated from particles size-selected at 30 nm and the first peak for 50 nm and 80 nm; L-Valine + 2MGA 2 was calculated from the second peak of particles size-selected at 50 nm and 80 nm.

The experimental Kappa values show that the mixture of proline and ammonium sulfate is moderately hygroscopic on the high end, with a Kappa of 0.50 ± 0.03 . The mixture of proline and 2MGA is moderately hygroscopic on the low end, with a Kappa of 0.21 ± 0.10 . The mixture of leucine and ammonium sulfate is moderately hygroscopic on the low end, with a Kappa of

0.29 ± 0.13 . The mixture of leucine and 2MGA is non-hygroscopic, with a Kappa of -0.04 ± 0.04 . The mixture of valine and ammonium sulfate is moderately hygroscopic on the low end, with a Kappa of 0.27 ± 0.12 . For the mixture of valine and 2MGA, the same trend of two adjacent peaks was observed as the pure valine. For smaller sizes, the mixture is non-hygroscopic with a Kappa of -0.08 ± 0.07 , while for larger sizes, the mixture is moderately hygroscopic on the low end, with a Kappa of 0.29 ± 0.07 . Although theoretically Kappa values can not be negative, it is possible that the experimental and calculation models can not accurately capture the true Kappa when the particle shape is far away from the assumed spherical shape and when the dry non-spherical particles rearrange and shrink in size to become spherical when absorb water.

The Kappa for each mixture and their pure compound components were plotted on the same graph to determine whether a trend is present between the Kappa values for pure components and their mixture, as shown in **Figure 15 - 20**.

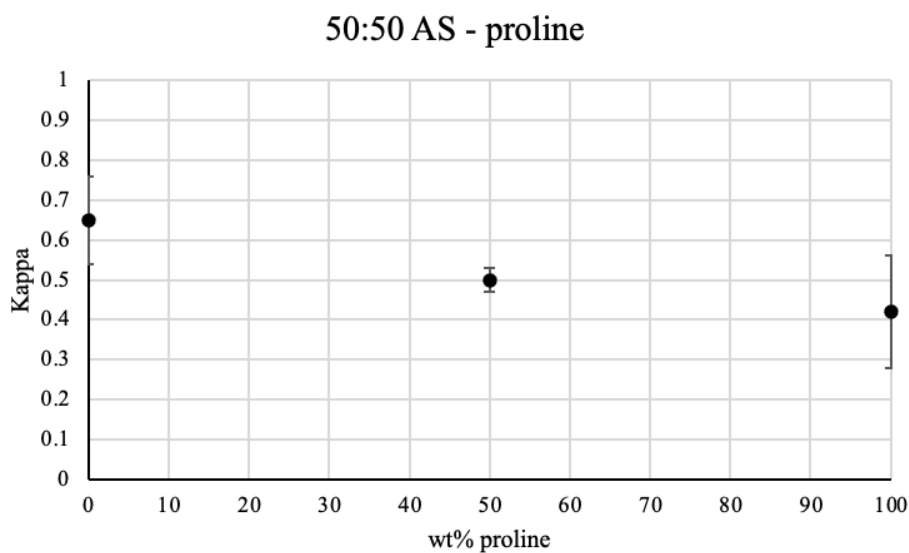


Figure 15. Kappa plot for Proline + AmmSulf mixture and its pure components, where 0 wt% proline means pure ammonium sulfate, 50 wt% proline means 50:50 mixture, and 100wt% proline means pure proline. The error bars represent one standard deviation.

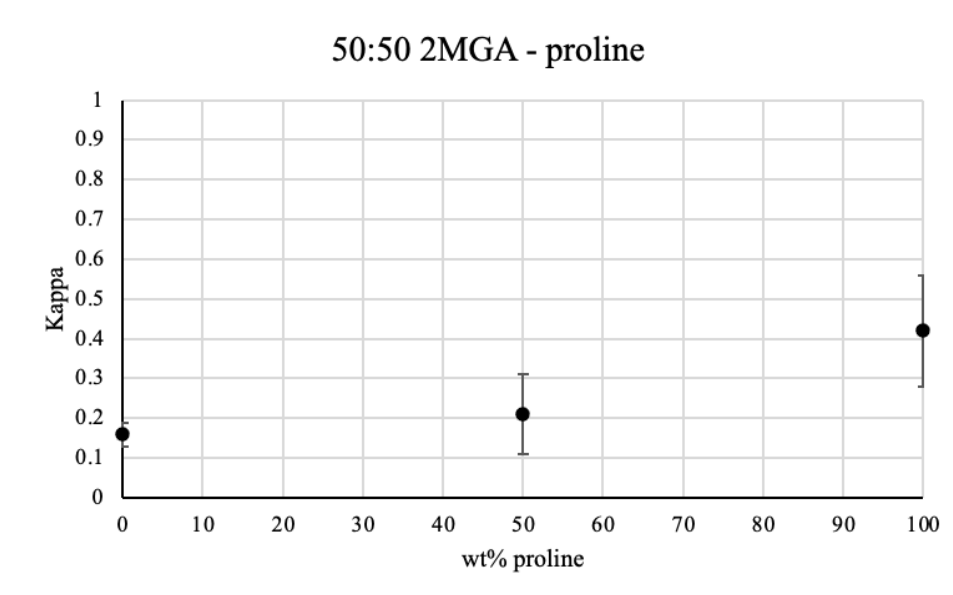


Figure 16. Kappa plot for Proline + 2MGA mixture and its pure components, where 0 wt% proline means pure 2MGA, 50 wt% proline means 50:50 mixture, and 100wt% proline means pure proline. The error bars represent one standard deviation.

For the mixture of proline and ammonium sulfate, as shown in **Figure 15**, the Kappa value for the mixture is in between the individual components Kappa values. Same for the mixture of proline and 2MGA, shown in **Figure 16**, the mixture Kappa value is in between the individual components Kappa values. This indicates that the mixture of two hygroscopic particles remains to be hygroscopic.

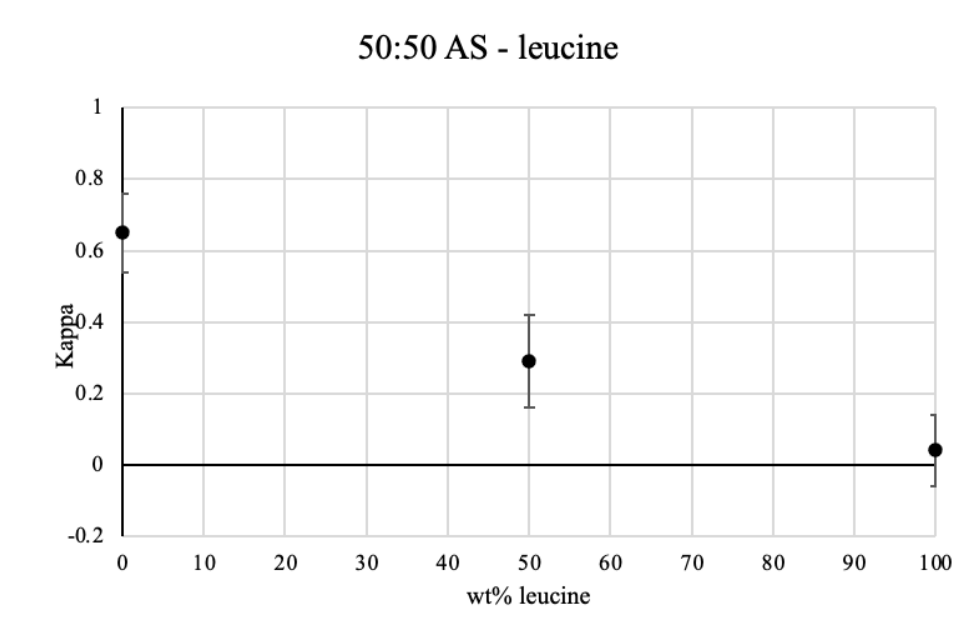


Figure 17. Kappa plot for Leucine + AmmSulf mixture and its pure components, where 0 wt% leucine means pure ammonium sulfate, 50 wt% leucine means 50:50 mixture, and 100wt% leucine means pure leucine. The error bars represent one standard deviation.

For the mixture of leucine and ammonium sulfate, as shown in **Figure 17**, the Kappa value for the mixture is also in between the individual components Kappa values. This shows that the mixture of a highly hygroscopic particle and a non-hygroscopic particle could be slightly hygroscopic.

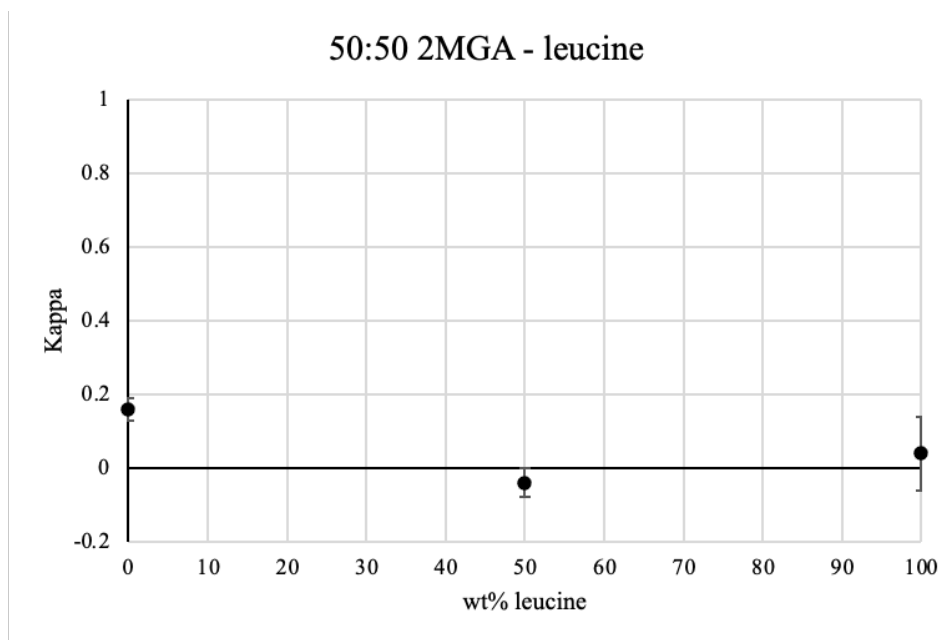


Figure 18. Kappa plot for Leucine + 2MGA mixture and its pure components, where 0 wt% leucine means pure 2MGA, 50 wt% leucine means 50:50 mixture, and 100wt% leucine means pure leucine. The error bars represent one standard deviation.

For the mixture of leucine and 2MGA, as shown in **Figure 18**, no obvious trend is observed for the Kappa values of the mixture and individual components, while the results show that the mixture of one non-hygroscopic particle and one slightly hygroscopic particle could remain non-hygroscopic.

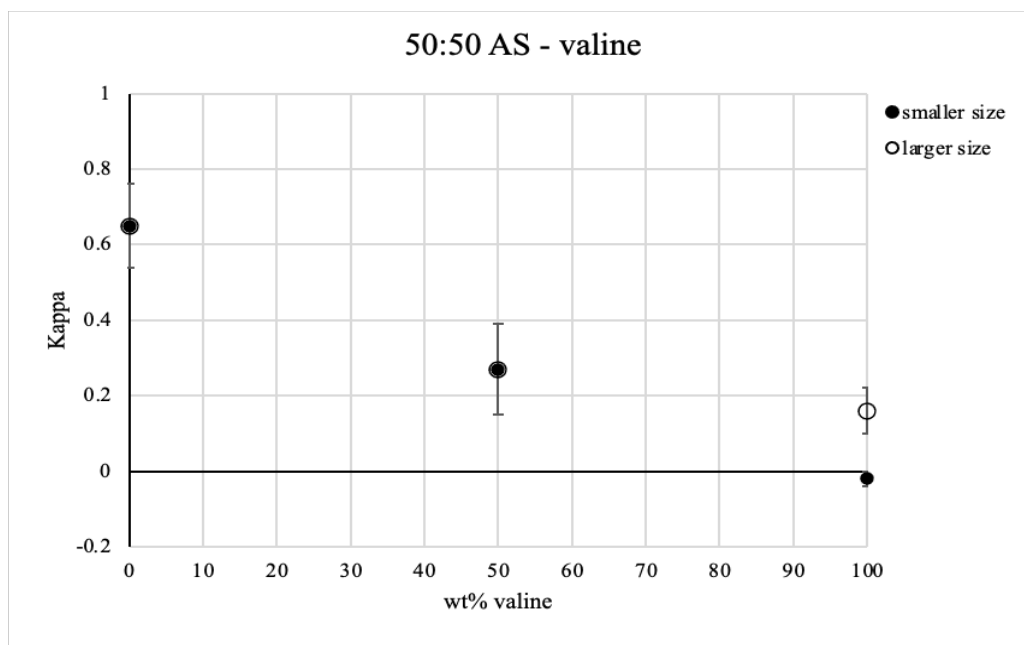


Figure 19. Kappa plot for Valine + AmmSulf mixture and its pure components, where 0 wt% valine means pure ammonium sulfate, 50 wt% valine means 50:50 mixture, and 100wt% valine means pure valine. The error bars represent one standard deviation, and the solid dots are for larger-size mixture and the hollow dots are for smaller-size mixture.

For the mixture of valine and ammonium sulfate, as shown in **Figure 19**, the Kappa value for the mixture is in between the individual components' Kappa values, for both large sizes and smaller sizes. This shows that the mixture of a highly hygroscopic particle and a non-hygroscopic particle could be slightly hygroscopic.

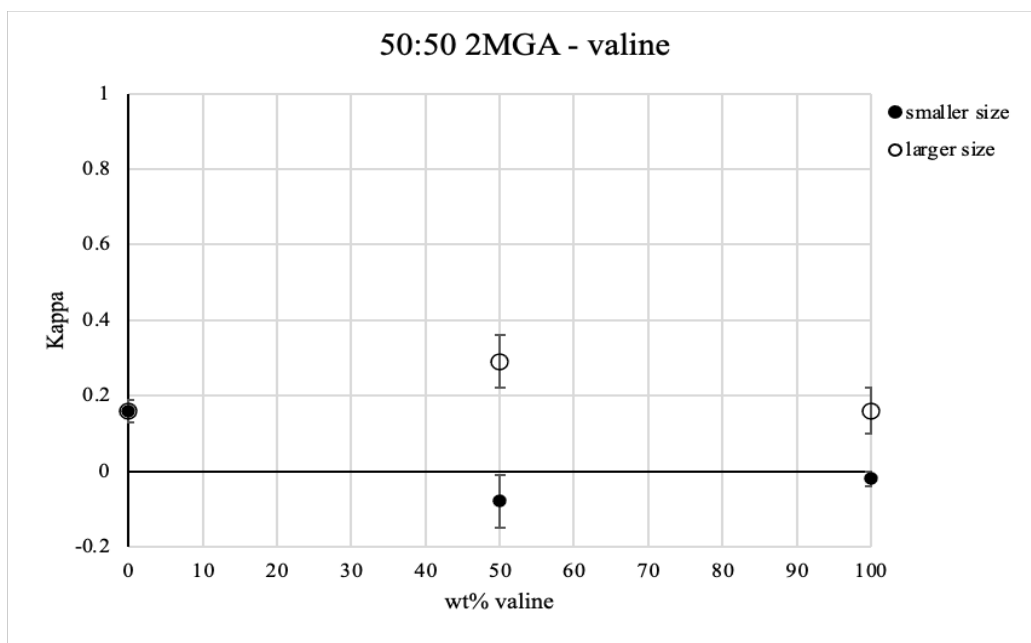


Figure 20. Kappa plot for Valine + 2MGA mixture and its pure components, where 0 wt% valine means pure 2MGA, 50 wt% valine means 50:50 mixture, and 100wt% valine means pure valine. The error bars represent one standard deviation, and the solid dots are for larger-size mixture and the hollow dots are for smaller-size mixture.

For the mixture of valine and 2MGA, as shown in **Figure 20**, no obvious trend is observed for the Kappa values of the mixture and individual components, while the results show that the mixture of one non-hygroscopic particle and one slightly hygroscopic particle could remain either non-hygroscopic or slightly hygroscopic.

Conclusions and Future work

In conclusion, an HTDMA system with RH control system was successfully built, tested, and calibrated in this study. Several organic aerosols and mixtures were studied for the first time using the designed HTDMA. This is a big accomplishment for myself, for the air quality research lab's future projects, and for the researchers in the aerosol field. The lab HTDMA system can be used for future hygroscopicity studies on a variety of chemical compounds at desired relative humidity conditions. However, due to the limited shared lab space, some tubing connections are too long or too short, causing the flow to have potential leaks or pressure drops, affecting the overall accuracy of the system. Future experimentalists in our lab will need to check and calibrate the system every couple of months before collecting data. Improvements in balancing the flows and ensuring non-leaking flowlines might help to increase the accuracy of the system. These initial growth factors and Kappa values on pure compounds and mixtures could also be served as references for future researchers.

Initial results indicate that L-proline is moderately hygroscopic, L-leucine is non-hygroscopic, L-valine is only slightly hygroscopic for larger sizes, and 2-Methylglutaric Acid (2MGA) is only slightly hygroscopic. The mixture of proline and ammonium sulfate is moderately hygroscopic on the high end over all other mixtures. The mixtures of proline + 2MGA, leucine + ammonium sulfate, valine + ammonium sulfate are moderately hygroscopic on the low end. The mixture of leucine and 2MGA is non-hygroscopic. For the mixture of valine and 2MGA, smaller sizes are non-hygroscopic, while larger sizes are moderately hygroscopic on the low end. The results also show that a mixture of two hygroscopic particles could remain to be hygroscopic; a mixture of a highly hygroscopic particle and a non-hygroscopic particle could be

slightly hygroscopic; and mixture of one non-hygroscopic particle and one slightly hygroscopic particle could remain either non-hygroscopic or slightly hygroscopic.

Although some findings were observed based on the initial results, more experiments are required to increase the repeatability of these results and to be more accurate and conclusive on the hygroscopic properties of studied aerosol particles. Especially for L-valine, more repeated runs at different sizes and RH conditions should be performed to determine if the observed two different growths are real and meaningful. In the future, firstly, more runs will be conducted at a wider range of relative humidity from 30 % to 90% for each individual compound to have a more accurate characterization of the hygroscopicity of pure compound. Additionally, more runs will be conducted at a wider range of relative humidity from 30 % to 90% for each mixture. Lastly, different weight percentage ratio of mixture such as 10:90, 30:70, 70:30 and 90:10 will be studied to have a broader understanding of hygroscopic behaviors for mixtures.

Bibliography

- Brechtel, F. J., & Kreidenweis, S. M. (2000). Predicting Particle Critical Supersaturation from Hygroscopic Growth Measurements in the Humidified TDMA. Part II: Laboratory and Ambient Studies. *Journal of The Atmospheric Sciences*, volume 75, 1872-1887.
- Banavar, J. R., & Maritan, A. (2010). Coalescence and fragmentation. *Annual Review of Condensed Matter Physics*, 1(1), 307-328. <https://doi.org/10.1146/annurev-conmatphys-070909-103925>
- Cruz, C. N., & Pandis, S. N. (2000). Deliquescence and hygroscopic growth of mixed inorganic–organic atmospheric aerosol. *Environmental Science & Technology*, 34(20), 4313–4319. <https://doi.org/10.1021/es9907109>
- Fuchs, N. A. (1989). *The mechanics of aerosols*. Dover Publications.
- Kreidenweis, S.M., and A. Asa-Awuku. (2014). Aerosol Hygroscopicity: Particle Water Content and Its Role in Atmospheric Processes. *Treatise on Geochemistry*, pp. 331–361., <https://doi.org/10.1016/b978-0-08-095975-7.00418-6>.
- Koehler, H. (1936). The nucleus in and the growth of hygroscopic droplets. *Transactions of the Faraday Society*, 32, 1152-1161. doi:10.1039/tf9363201152
- Moore, R. H., and T. M. Raymond (2008), HTDMA analysis of multicomponent dicarboxylic acid aerosols with comparison to UNIFAC and ZSR, *J. Geophys. Res.*, 113, D04206, doi:10.1029/2007JD008660.
- Mulholland, G. W., Donnelly, M. K., Hagwood, C. R., Kukuck, S. R., Hackley, V. A., & Pui, D. Y. (2006). NIST reference materials for particle size measurement. *Journal of research of the National Institute of Standards and Technology*, 111(2), 89-104.

- Petters, M. D., & Kreidenweis, S. M. (2007). A single parameter representation of hygroscopic growth and cloud condensation nucleus activity. *Atmospheric Chemistry and Physics*, 7(8), 1961-1971. doi:10.5194/acp-7-1961-2007
- Rader, D. J., & McMurry, P. H. (1986). Application of the tandem differential mobility analyzer to studies of droplet growth or evaporation. *Journal of Aerosol Science*, 17(5), 771–787. [https://doi.org/10.1016/0021-8502\(86\)90031-5](https://doi.org/10.1016/0021-8502(86)90031-5).
- Sorooshian, A., Padró, L. T., Nenes, A., Feingold, G., McComiskey, A., Hersey, S., ... & Wang, Z. (2009). On the link between ocean biota emissions, aerosol, and maritime clouds: Airborne, ground, and satellite measurements off the coast of California. *Global Biogeochemical Cycles*, 23(2).
- Tang, M., Chan, C. K., Li, Y. J., Su, H., Ma, Q., Wu, Z., Zhang, G., Wang, Z., Ge, M., Hu, M., He, H., & Wang, X. (2019). A review of experimental techniques for Aerosol Hygroscopicity Studies. *Atmospheric Chemistry and Physics*, 19, 12631–12686. <https://doi.org/10.5194/acp-19-12631-2019>
- Taylor, N. F., Collins, D. R., Spencer, C. W., Lowenthal, D. H., Zielinska, B., Samburova, V., & Kumar, N. (2011). Measurement of ambient aerosol hydration state at Great Smoky Mountains National Park in the Southeastern United States. *Atmospheric Chemistry and Physics*, 11(23), 12085–12107. <https://doi.org/10.5194/acp-11-12085-2011>.
- Wang, J., et al. (2011). Differential mobility analyzer: A review of particle sizing techniques for measuring fine and ultrafine particles. *Journal of Aerosol Science*, 42(5), 307-326.

Appendix

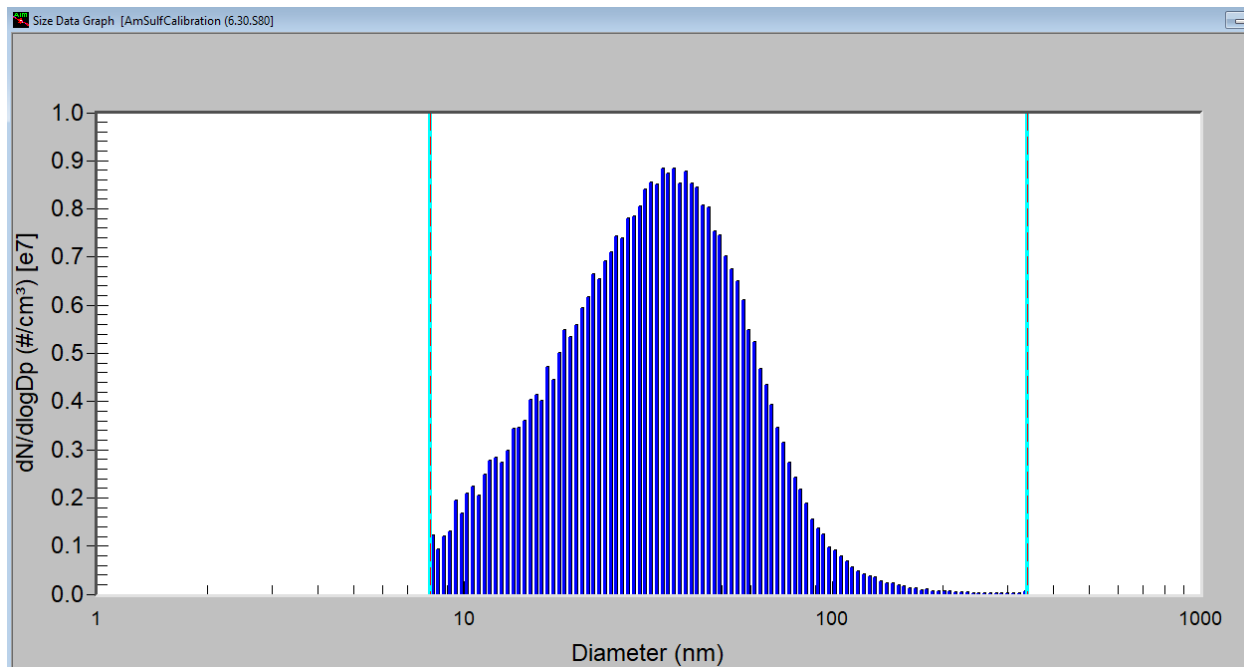


Figure A1. Full-size distribution of ammonium sulfate at 0.1 g/L obtained from DMA, where the sheath flow rate is 8 lpm and the sample flow rate is 0.3 lpm (which is a typical operating condition).

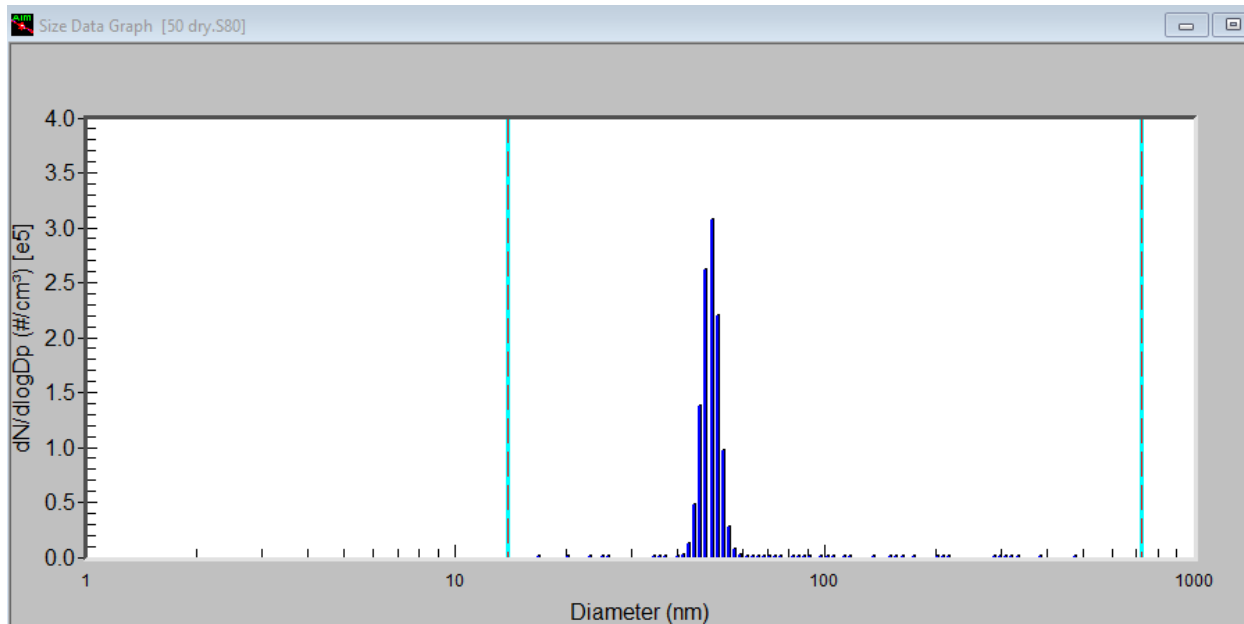


Figure A2. Selected narrow-range size distribution of ammonium sulfate (0.1 g/L) obtained from TDMA, where the size is selected at 50 nm on the first DMA and the sheath flow rate is at 3 lpm while sample flow rate is at 0.3 lpm for both DMAs.